Crystal Structure of *Nitrosomonas europaea* Cytochrome *c* Peroxidase and the Structural Basis for Ligand Switching in Bacterial Di-heme Peroxidases†

Hideaki Shimizu,[‡,§] David J. Schuller,[‡,§,||] William N. Lanzilotta,[‡,§,⊥] M. Sundaramoorthy,[‡,#] David M. Arciero,[▽,◆] Alan B. Hooper,[▽] and Thomas L. Poulos*[,‡]

Department of Molecular Biology & Biochemistry, Department of Physiology & Biophysics, and Program in Macromolecular Structure, University of California, Irvine, California 92697-3900, and Department Biochemistry, Molecular Biology, and Biophysics, University of Minnesota, St. Paul, Minnesota 55108

Received July 16, 2001; Revised Manuscript Received August 13, 2001

ABSTRACT: The crystal structure of the fully oxidized di-heme peroxidase from *Nitrosomonas europaea* has been solved to a resolution of 1.80 Å and compared to the closely related enzyme from *Pseudomonas aeruginosa*. Both enzymes catalyze the peroxide-dependent oxidation of a protein electron donor such as cytochrome *c*. Electrons enter the enzyme through the high-potential heme followed by electron transfer to the low-potential heme, the site of peroxide activation. Both enzymes form homodimers, each of which folds into two distinct heme domains. Each heme is held in place by thioether bonds between the heme vinyl groups and Cys residues. The high-potential heme in both enzymes has Met and His as axial heme ligands. In the *Pseudomonas* enzyme, the low-potential heme has two His residues as axial heme ligands [Fulop et al. (1995) *Structure 3*, 1225−1233]. Since the site of reaction with peroxide is the low-potential heme, then one His ligand must first dissociate. In sharp contrast, the low-potential heme in the *Nitrosomonas* enzyme already is in the "activated" state with only one His ligand and an open distal axial ligation position available for reaction with peroxide. A comparison between the two enzymes illustrates the range of conformational changes required to activate the *Pseudomonas* enzyme. This change involves a large motion of a loop containing the dissociable His ligand from the heme pocket to the molecular surface where it forms part of the dimer interface. Since the *Nitrosomonas* enzyme is in the active state, the structure provides some insights on residues involved in peroxide activation. Most importantly, a Glu residue situated near the peroxide binding site could possibly serve as an acid−base catalytic group required for cleavage of the peroxide O−O bond.

Cytochrome *c* peroxidases (CCPs)[1] catalyze the oxidation of ferrocytochrome *c* and reduction of H_2O_2 in the following reaction:

$$2\text{cyt.}c(Fe^{2+}) + H_2O_2 + 2H^+ \rightarrow 2\text{cyt.}c(Fe^{3+}) + 2H_2O$$

Although yeast cytochrome *c* peroxidase (CCP) is the best known and most well-studied CCP (*1*), CCP also is found in various prokaryotes such as *Pseudomonas aeruginosa* (*2*, *3*), *Paracoccus denitrificans* (*4*), *Rhodobacter capsulatus* (*5*), and *Nitrosomonas europaea* (*6*). Of these, the *Ps. aeruginosa* CCP is the most thoroughly investigated including the only one of this family for which a crystal structure has been determined (*7*). Close sequence similarities, molecular weight, and heme content indicate that the general structural features found in the *Ps. aeruginosa* CCP will be conserved in the other prokaryotic CCPs. The most notable difference between the prokaryotic and eukaryotic peroxidases is that the single polypeptide chain consisting of ≈300 residues contains 2 hemes both of which are covalently tethered to the protein via thioether links between the heme vinyl groups and Cys residues as in *c*-type cytochromes. In contrast, eukaryotic peroxidases contain only one noncovalently bound heme. In the di-heme peroxidases, one heme has been termed high-potential and contains His and Met residues as axial heme ligands. The other, low-potential heme is considered to be the site of H_2O_2 activation, so one axial heme coordination position must be available for interaction with the incoming peroxide. However, the *Ps. aeruginosa* structure shows that the low-potential heme contains two His residues as axial ligands, leading to the proposal that one His ligand dissociates in order to enable peroxide to bind (*7*).

While the overall reaction for the di-heme peroxidases is similar to eukaryotic peroxidase, the catalytic intermediates are quite different. The traditional yeast CCP mechanism

† This work was supported by grants from the National Science Foundation (MCB-9723608 to A.B.H. and MCB-9807798 to T.L.P.).

‡ University of California, Irvine.

§ These authors contributed equally to this work.

|| Current address: Department of Molecular Biology & Genetics, 209 Biotechnology Building, Cornell University, Ithaca, NY 14853.

⊥ Current address: University of Georgia, Department of Biochemistry and Molecular Biology, Room A130, Life Sciences Building, Athens, Georgia 30602-7229. Phone: (706) 542-1573.

Current address: Department of Biochemistry & Molecular Biology, University of Kansas Medical Center, Kansas City, KS 66160-7421.

▽ University of Minnesota, St. Paul.

◆ Current address: R and D Systems, Inc., 614 McKinley, Minneapolis, MN 55413.

[1] Abbreviations: CCP, cyctochrome *c* peroxidase; PAP, *Ps. aeruginosa* di-heme peroxidase; NEP, *N. europaea* di-heme peroxidase; MAD, multiwavelength anomalous dispersion; hp, high-potential; lp, low-potential; cyt.*c*, cytochrome *c*.

10.1021/bi011481h CCC: $20.00
Published on Web 10/17/2001

proceeds in the following three steps:

$$Fe^{3+}\ Trp + H_2O_2 \rightarrow \underset{\text{Compound I}}{Fe^{4+}{-}O\ Trp^{\bullet+}} + H_2O$$

$$\underset{\text{Compound I}}{Fe^{4+}{-}O\ Trp^{\bullet+}} + \text{cyt.}c\ (Fe^{2+}) \rightarrow \underset{\text{Compound II}}{Fe^{4+}{-}O\ Trp} + \text{cyt.}c\ (Fe^{3+})$$

$$\underset{\text{Compound II}}{Fe^{4+}{-}O\ Trp} + \text{cyt.}c\ (Fe^{2+}) \rightarrow Fe^{3+}\ Trp + \text{cyt.}c\ (Fe^{3+}) + H_2O$$

In the first step, peroxide reacts with the enzyme to give Compound I. This oxidation/reduction reaction generates an $Fe^{4+}{-}O$ center and a cation radical centered on Trp191 (*8*). In other eukaryotic peroxidases, the porphyrin is oxidized to a cation radical rather than an amino acid side chain (*9*). Compound I is then reduced to Compound II followed by a second electron-transfer step that reduces Compound II back to the resting state. Again, other peroxidases follow the same process except the reducing substrate normally is an aromatic phenol rather than cyt.*c*.

The di-heme *Ps. aeruginosa* enzyme differs in how oxidizing equivalents are stored. The high-potential heme must be reduced to Fe^{2+} by either ferrocyt.c_{551} or the Cu^{1+} in azurin in order for the enzyme to function (*10*). The

Table 1: Data and Refinement Statistics[a]

Data Statistics

wavelength (Å)	resolution, $I/\sigma I$ (Å)	no. obsd	completeness (%)	unique reflections	R_{sym}[b]
1.7382 edge	2.50	441576	44173	94.6 (57.3)	0.137 (0.297)
	7.9				
1.7407 inflection	2.60	361371	41069	97.9 (77.9)	0.206 (0.459)
	6.3				
1.5498 remote	2.50	356375	45927	100.0 (100.0)	0.113 (0.490)
	6.6				
1.00 used for refinement	1.80	393924	119903	96.0 (89.1)	0.031 (0.130)

Refinement Statistics

protein non-H atoms	3322
solvent molecules	859
resolution range (Å)	50.0−1.8
total reflections	113854
total reflections used in R_{free}	6036
R_{cryst}	0.222
R_{free}	0.257
rmsd of bond distances (Å)	0.007
rmsd of bond angles (deg)	1.37

[a] Numbers in parentheses are for the highest resolution, which for the native data set used for refinement is 1.86−1.79 Å. MAD data were collected at the Advanced Light Source beamline 5.0.2. [b] $R_{sym} = \sum_{hkl,i}(|I_{hkl,i} - \langle I_{hkl}\rangle|)/\sum_{hkl,i}\langle I_{hkl}\rangle$, where I_{hkl} is the intensity of an individual measurement of the reflection with indices *hkl* and $\langle I_{hkl}\rangle$ is the mean intensity of that reflection.

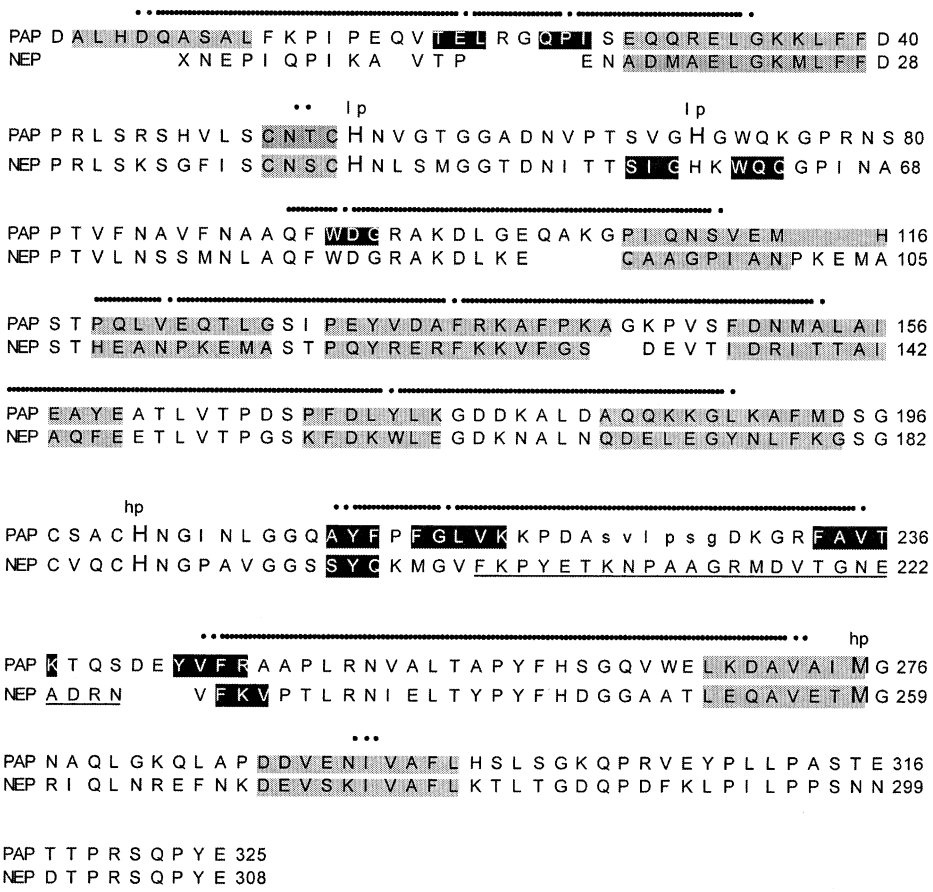

FIGURE 1: Structure-based sequence alignment of NEP and PAP. The gray regions are helical and the dark regions β-sheet. hp and lp denote high-potential and low-potential heme ligands, respectively. Residues in italics for PAP were not visible in the reported electron density maps (*7*), and the region underlined gives very poor structure-based alignment. Sequence identities are indicated by a vertical line.

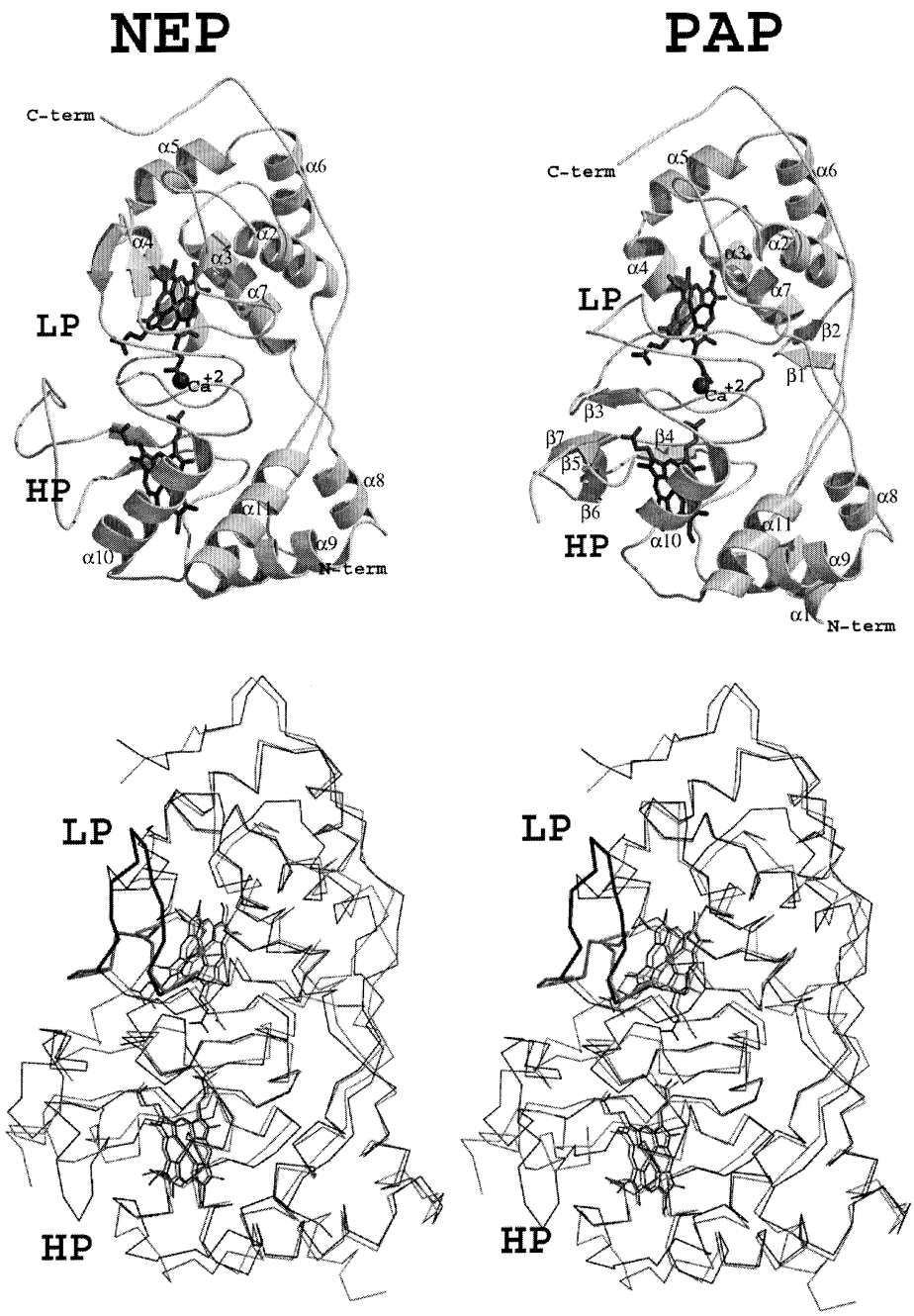

FIGURE 2: Models showing the NEP and PAP subunits. The top mono diagrams are single subunits of NEP and PAP with the various elements of secondary structure labeled. The bottom diagram is a stereoview showing superposition of NEP and PAP based on a least-squares fit of Cα atoms. The stereo diagram is in the same orientation as the mono diagrams. The darker backbone trace is for PAP, and the His-ligand loop that differs between NEP and PAP is highlighted as the thicker line. Figures 3−6 were prepared with Bobscript (*23*, *24*) and Raster3D (*25*).

mechanism shown below is taken from Greenwood et al. (*11*):

$$\underset{\text{high low}}{Fe^{2+}\,Fe^{3+}} + H_2O_2 \rightarrow \underset{\text{high low}}{Fe^{3+}\,Fe^{4+}{=}O} + H_2O$$

Compound I

$$\underset{\text{high low}}{Fe^{3+}\,Fe^{4+}{=}O} + e^- \rightarrow \underset{\text{high low}}{Fe^{3+}\,Fe^{3+}} + H_2O$$

Compound II

$$\underset{\text{high low}}{Fe^{3+}\,Fe^{3+}} + e^- \rightarrow \underset{\text{high low}}{Fe^{2+}\,Fe^{3+}}$$

Compound II

In this case, the high-potential heme serves the function of the Trp191 radical in yeast CCP and carries one peroxide-derived oxidizing equivalent. This requires intramolecular electron transfer from the high- to low-potential heme. Since both hemes are tethered to the same polypeptide, the di-heme peroxidases offer distinct advantages in studying the details of intramolecular electron transfer since the structural uncertainties in protein−protein interactions are not an issue.

The *N. europaea* di-heme peroxidase also has been characterized (*6*). While exhibiting striking similarities to the *Ps. aeruginosa* enzyme, the values of the reduction potential of the high- and low-potential hemes of the *N.*

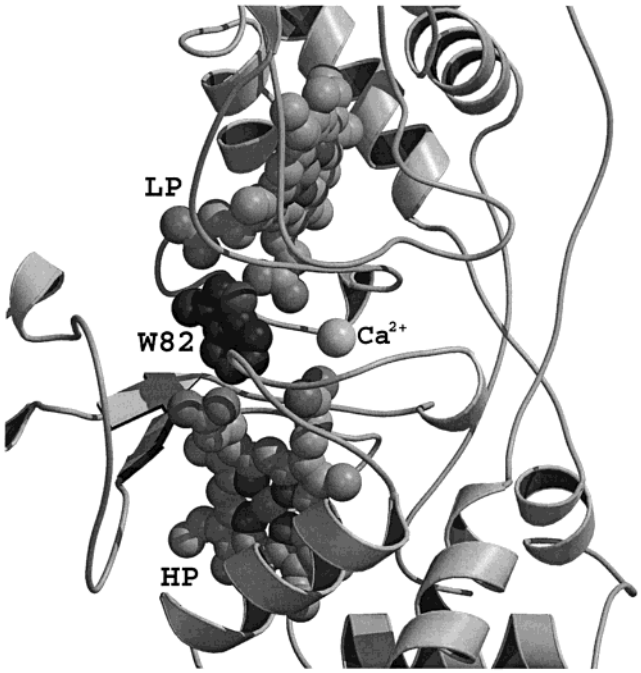

FIGURE 3: Close-up view of the region between the two hemes. Note that Trp82 contacts both heme propionates as in the PAP di-heme peroxidase, which could provide an electron-transfer conduit between the two hemes (*7*).

europaea enzyme were found to be 130 and 70 mV, respectively, higher than the *Ps. aeruginosa* hemes. Further, the *N. europaea* enzyme was found to react with H_2O_2 in the fully oxidized or half-reduced states as opposed to the *Ps. aeruginosa* enzyme, which must first have the high-potential heme reduced (*10*). Thus, the resting *N. europaea* and *Ps. aeruginosa* enzymes differ in reactivity with H_2O_2 and in the nature of the way oxidizing equivalents from H_2O_2 are stored after formation of the ferryl oxygen derivative. In the diferric *N. europaea* enzyme, the spectral data indicate a porphyrin radical similar to traditional heme peroxidases (*6*). To probe the structural basis for this difference as well as to shed further light on the possible role that ligand displacement might play in the catalytic mechanism, we have determined the crystal structure of the di-heme peroxidase from *N. europaea*.

MATERIALS AND METHODS

NEP was purified and the oxidized enzyme crystallized as described previously (*6, 12*). Crystals belong to space group $P2_1$ with $a = 88.13$ Å, $b = 55.11$ Å, $c = 144.0$ Å, and $\beta = 103.6°$ with a dimer of dimers (four subunits) per asymmetric unit. MAD data at the iron edge, at the inflection point, and at a remote wavelength were collected at the Advanced Light Source, beamline 5.0.2. Initial phases were obtained using molecular replacement methods and the PAP crystal structure (*7*). A poly-alanine model of the PAP subunit including both hemes, the single calcium, and residues 1−222 and 229−323 was used as the probe. The initial search was carried out with AMoRe (*13*) at 5 Å resolution. The best rotation/translation solution was rigid-body-refined and fixed in place followed by searches for the remaining molecules in the asymmetric unit. A total of four solutions were found, corresponding to the expected two dimers per asymmetric unit. The final *R* factor was 52.6% with a correlation coefficient of 37.3%. The heme iron atoms were located using a MAD data set and phases calculated using SHARP (*14*). The MAD and molecular replacement phases were combined, and modified with solvent flattening, histogram matching, and 4-fold density averaging (*15*) as implemented in the CCP4 package (*16*). The resulting electron density maps were used to fit the NEP sequence

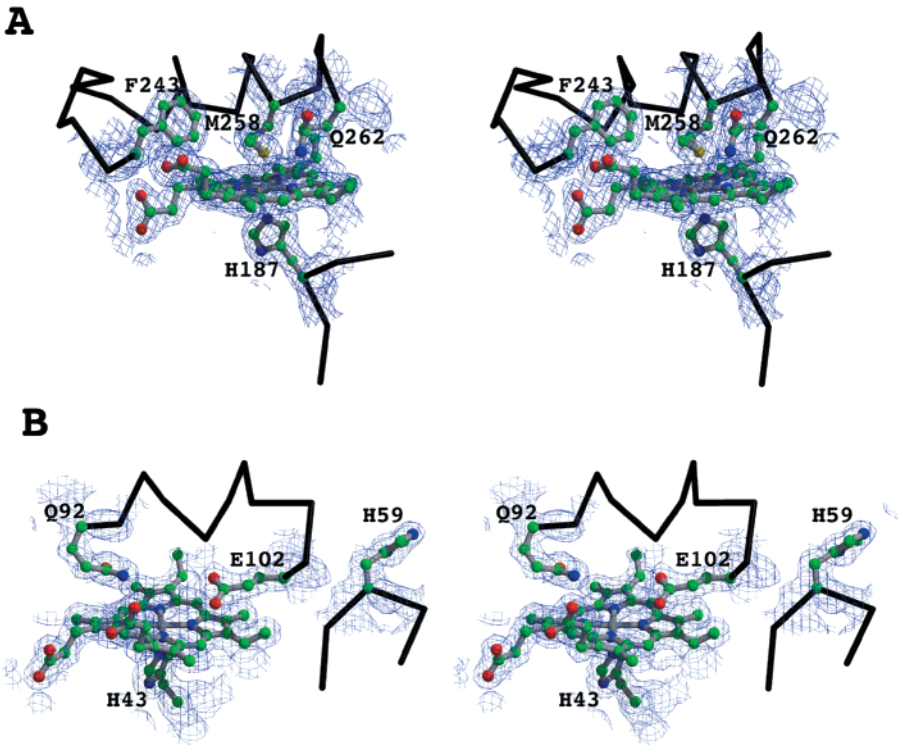

FIGURE 4: Stereo diagram of the composite $2F_o-F_c$ omit electron density maps around the two hemes contoured at 1.0σ. (A) High-potential heme; (B) low-potential heme.

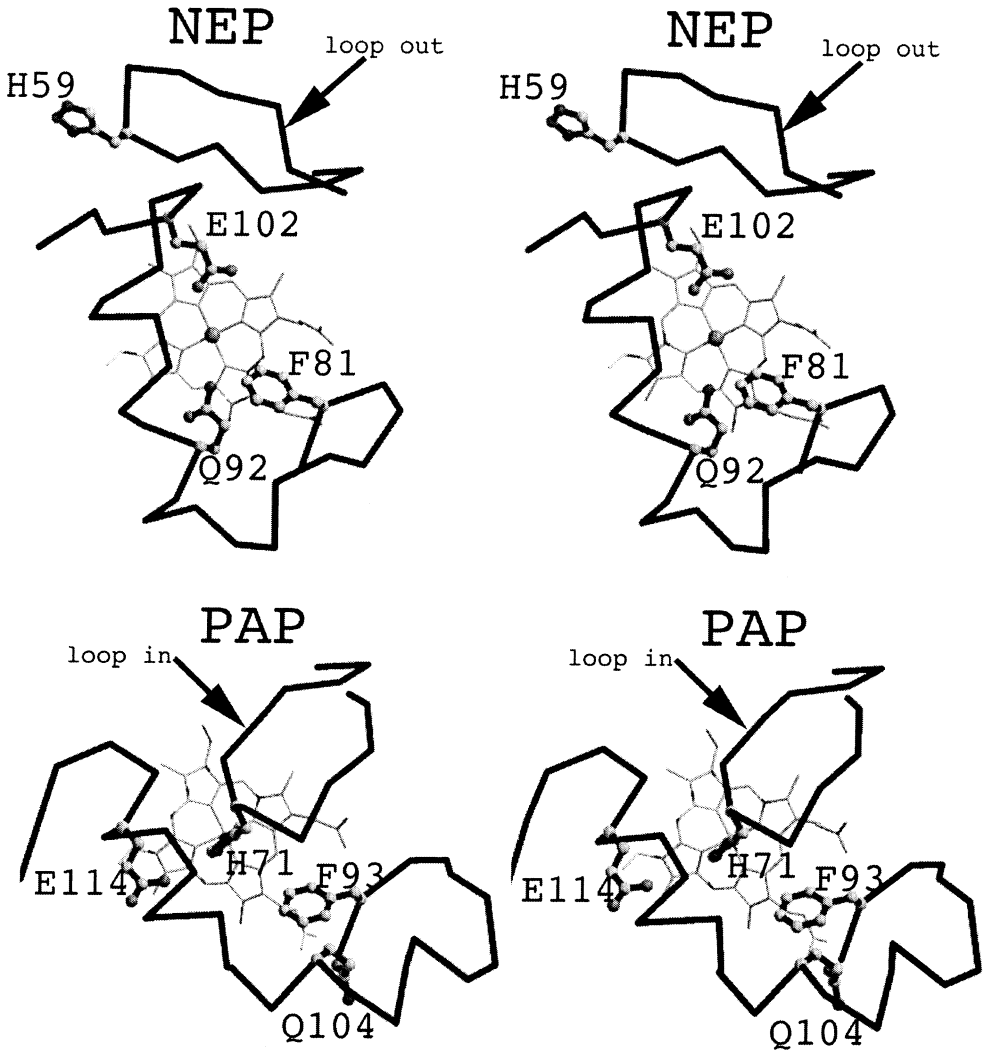

FIGURE 5: Stereo diagrams showing a comparison between NEP and PAP around the ligand binding environment of the low-potential heme. In PAP, His71 is a heme ligand while the corresponding residue in NEP, His59, is situated out on the surface of the molecule, leaving the distal coordination position available for reaction with peroxide. Presumably PAP must adopt a conformation similar to NEP in order to be active as a peroxidase.

followed by iterative rounds of refinement using CNS (*17*) and model building using TOM (*18*). In the early stages of refinement, noncrystallographic symmetry restraints were applied but were removed in the later stages of refinement. Prior to completion of the refinement, the raw native data set was reprocessed with MOSFLM (http://www.dl.ac.uk/CCP/CCP4/dist/html/mosflm.html). A summary of the final refinement statistics is given in Table 1.

RESULTS AND DISCUSSION

Overall Structure. NEP is a dimer in solution (*6*), and the NEP crystals contain two dimers in the asymmetric unit. One subunit (subunit D) was particularly troublesome during model building and refinement owing to poorly defined electron density. This is evidenced by the higher thermal (*B*) factors for subunit D. In what follows, we focus on the A−B dimer pair since this has the best resolved electron density. The structure-based sequence alignment between PAP and NEP is shown in Figure 1. As expected, the overall structure of NEP is very similar to PAP with all the helices except α1 being conserved (Figures 1 and 2). NEP is slightly shorter, 308 residues compared to 325 in PAP. Part of the difference is at the N-terminal segment where PAP begins with a helix while NEP is six residues shorter and does not have the N-terminal helix. Other differences are primarily in surface regions including β1 and β2, residues 19−21 and 24−26, which form a loop on the surface of PAP and are missing in NEP. Despite these differences, the close similarity in structures is underscored by an rms deviation = 1.55 Å for 250 common Cα atoms.

The subunit folds into two distinct domains with the fold of each domain closely resembling that found in class 1 *c*-type cytochromes. Each domain houses one heme which has been designated the high- and the low-potential heme (abbreviated lp and hp, respectively). The closest approach of the two hemes is ≈10 Å although the heme propionates are directly bridged by the indole ring of Trp82 (Figure 3). This interaction is the same as in Trp94 of PAP and as was noted by Fulop et al. (*7*) is a possible electron-transfer conduit between the two hemes (Figure 3).

The lp domain (15−146) and hp domain (146−280) are bridged by interdomain regions 1−15, 147−153, and 280−308. Residues 69−91 and 227−250 form the interdomain interface and also sandwich a divalent cation in place at the

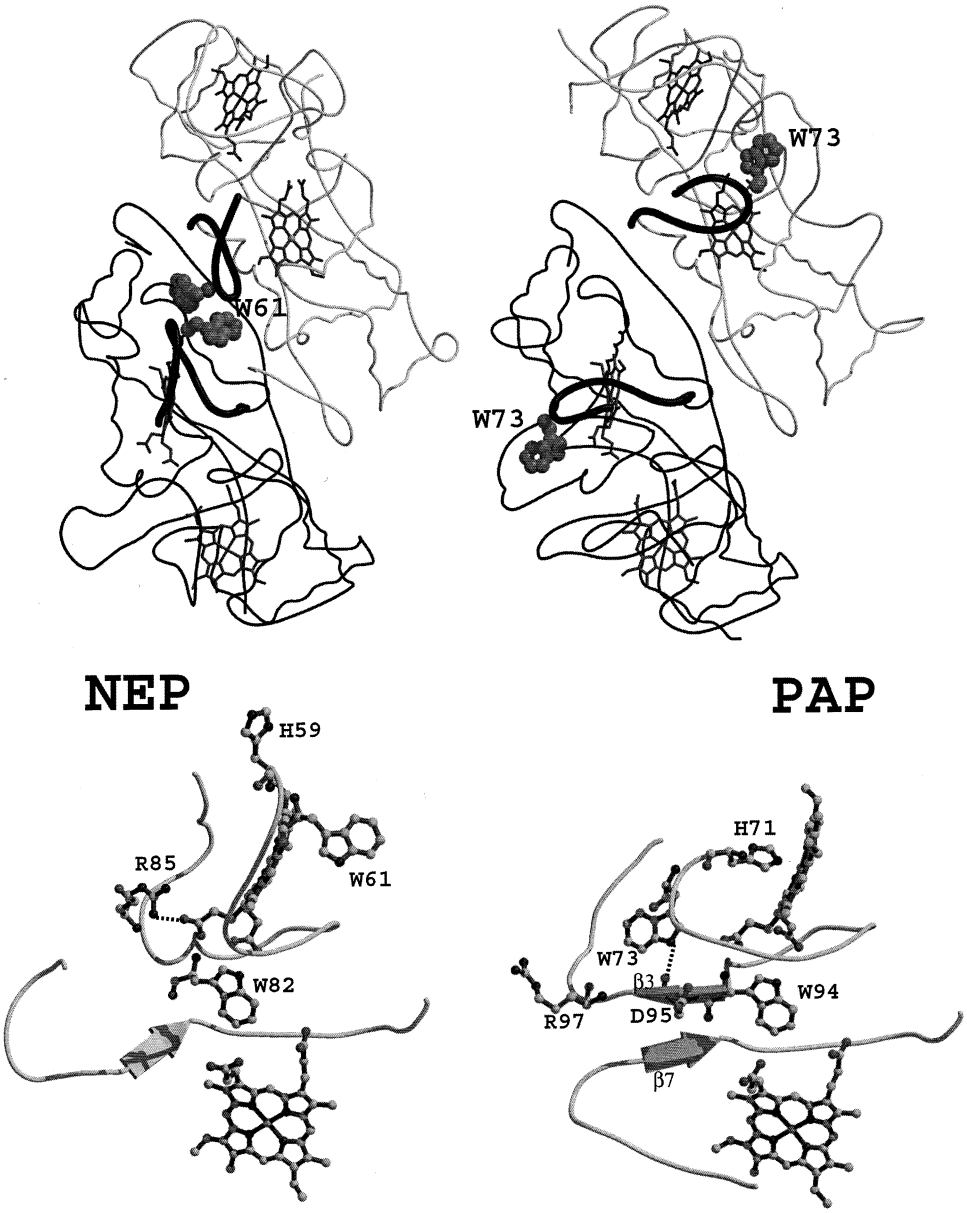

FIGURE 6: Comparison of the NEP and PAP dimers and the interdomain interface. The dimers in the top diagrams show the high-potential ligand "activation" loop highlighted as the thick line. In NEP, Trp61 forms contacts at the dimer interface with its symmetry-related mate. In PAP, the loop "in" conformation places the corresponding Trp, Trp73, close to the low-potential heme. The bottom diagrams provide a close-up view of the immediate environment at the domain interface within each subunit. In PAP, there is a well-defined beta pair between the domain while this feature is absent in NEP. Note the difference in positions of the corresponding Trp residues (Trp61 in NEP and Trp73 in PAP). This region of the structure might be involved in the redox-linked conformational changes required to displace His71 in PAP as a proximal ligand in order to make available a distal coordination position for reaction with peroxide.

dimer interface. This cation (Figure 3), most likely calcium (*7*), is also present in PAP. In both enzymes, the calcium is not coordinated by carboxylates but by solvent and peptide carbonyl oxygens although the calcium in NEP is about 4.6 Å from the hp heme propionate. The lp domain contains an important His59-containing loop (56−65) which differs between the two enzymes and will be discussed below.

Heme Environments. The hp heme is anchored to the protein via thioether bonds by Cys183 and Cys186 with the heme iron coordinated by His187 and Met258 (Figure 4A) just as in PAP. The lp heme also is anchored via thioether bonds. However, in comparing the PAP and NEP structures, the most striking difference is the environment around the low-potential heme (Figures 4B and 5). Unlike PAP which has two His residues coordinated to the heme, the NEP lp heme is pentacoordinate. Substantial conformational differences between the two enzymes in this region result in placement of His59 in NEP, corresponding to the His71 ligand in PAP, near the surface. The loop between residues 68 and 77 in PAP adopts an "in" conformation which enables His71 to coordinate the heme iron while the corresponding loop in NEP between residues 56 and 65 adopts the "out" conformation (Figure 5). The net result of the displacement of His59 is to make the heme pentacoordinate and hence reactive toward peroxides.

This difference in coordination environment also enables catalytically important residues to be positioned into the NEP heme pocket that is occupied by the His ligand in PAP. Both Glu102 and Gln92 (Glu114 and Gln104 in PAP, Figures 4 and 5) bracket the peroxide binding site and are in position

to interact with diatomic ligands. Hence, NEP lacks the distal side acid/base catalytic His found in other peroxidases. In other peroxidases, this catalytic distal His is essential for promoting heterolytic cleavage of the peroxide O−O bond. The closest homologue in NEP is Glu102, which could serve a similar function. The only other heme peroxidase known to use Glu as a catalytic group is chloroperoxidase (*19*). The Glu in chloroperoxidase is thought to operate as an acid−base catalyst which helps to promote heterolytic cleavage of the peroxide O−O bond to form Compound I (*20, 21*). The location of the catalytic Glu is remarkably similar in NEP and chloroperoxidase. The carboxylate in both contacts the surface of the heme, and the closest approach of a carboxylate O atom to the heme is, within experimental error, the same, ≈5 Å. Thus, Glu102 very likely serves the same role as that proposed for the catalytic Glu in chloroperoxidase. The same mechanism probably operates in PAP, but the redox-linked conformational change must first occur which removes His71 as a ligand and places Glu114 in position for catalysis.

Domain Interface. The interface between domains within the subunit is very similar in NEP and PAP except for those regions involved in the difference in coordination environment of the lp heme (Figure 2). Most notably, residues 94−96 and 244−246 in PAP form a short antiparallel β-sheet (β_3, β_7) across the dimer interface. β7 also occurs in NEP, but the residues in NEP, 82−84, that correspond to β3 in PAP are oriented approximately perpendicular to the direction of the $\beta_3-\beta_7$ pair in PAP. The reorientation of residues 82−84 of NEP relative to PAP places this segment closer to the distal side of the lp heme, which enables Arg85 in NEP to ion-pair with a low-potential heme propionate (Figure 6). The corresponding residue in PAP, Arg97, is oriented out in solution. Therefore, the loss of hydrogen bonding in the β-sheet in going from PAP to NEP might be partially compensated for by the Arg85−heme propionate interactions.

Dimer Interactions. Both NEP and PAP crystallized as a dimer, but NEP forms noncrystallographic and PAP forms crystallographic dimers. Nevertheless, both peroxidases form the same dimer with variations due only to structural differences responsible for the changes in the low-potential heme coordination environment. This difference is due to the His ligand loop which is "out" in NEP and "in" in PAP (Figure 5). In NEP, this places the loop at the dimer interface where it interacts with its symmetry-related loop in the second subunit (Figure 6). The loop "out" conformation in NEP places Trp61 at the dimer interface, where it forms a stacking interaction with the 60−61 peptide bond and a 4.3 Å contact with Trp61 of the symmetry-related subunit (Figure 6). In contrast, the "in" position in PAP places the corresponding Trp in PAP, Trp73, about 3 Å from the low-potential heme propionate (Figure 6). In addition, the indole ring NH group H-bonds with the carbonyl O atom of Asp95 which is part of the unique antiparallel β-strand at the domain interface in PAP (Figure 6). Thus, in going from PAP to NEP, an H-bond and a partially interior position of the Trp are lost but are compensated for by new interactions at the dimer interface.

Structural Basis for the Ligand Switch. The comparison between NEP and PAP thus far suggests that, following reduction of the hp heme, PAP must undergo a structural change in the low-potential heme environment, resulting in a distal heme environment that resembles NEP (*7*). Thus, NEP may be thought of as being in the active state while PAP is inactive. Here it is important to note that NEP is fully active in the oxidized state while in PAP the high-potential heme first must be reduced. Since the fully oxidized PAP has His71 coordinated to the lp heme, reduction of the hp heme must result in the conformational changes required to give a pentacoordinate lp heme. Presumably this change results in the movement of the His71-ligand loop to the "out" position and subsequent formation of new dimer contacts as seen in NEP. Redox-induced conformational and ligand rearrangements have been observed before and are best documented in cytochrome cd_1 nitrite reductase (*22*). This enzyme also has two hemes, and upon reduction, the ligand environment of both hemes changes. Of particular relevance to our present work, the Tyr ligand of one heme is displaced upon reduction, which opens up a distal site for the required nitrite reduction chemistry (*22*). The parallels between the two enzymes are striking although the details and range of motions are quite different. In nitrite reductase, changes in the relative positioning of the two heme domains are large with a displacement of the *c*-heme being ≈6 Å. A least-squares superimposition of a PAP and NEP subunit shows that the relative positions of the two hemes are the same to within <1 Å. Thus, the redox-mediated conformational switches in PAP are confined to the local structure around the hp heme and not to any significant alterations in the relative position of the two heme domains.

Without the structure of the PAP in the half-reduced active state, explaining how reduction of the hp heme iron can lead to such changes in the lp heme remains rather speculative. However, one possibly important difference between NEP and PAP related to this problem is the quite different structures between the two hemes in the subunit. In PAP, residues 243−245, 210−212, and 94−97 form a short stretch of antiparallel β-sheet which connects the two hemes. The architecture in NEP is quite different and does not have as extensive an interaction between the two domains (Figure 6). Trp94 (Trp82 in NEP) is part of the PAP sheet structure and contacts both heme propionates (Figure 3) and could serve as a link between the two hemes. In addition to functioning as an electron-transfer conduit as suggested (*7*), this region of the structure including the sheet architecture might serve as a redox-linked conformational switch that leads to the rearrangement of the lp heme environment.

ACKNOWLEDGMENT

We are indebted to Dr. Vilmos Fulop for providing PAP coordinates which were used for molecular replacement.

REFERENCES

1. Poulos, T. L., and Fenna, R. (1994) *Met. Biol. 30*, 25−75.
2. Ellfolk, N., Ronnberg, M., Aasa, R., Andreasson, L. E., and Vanngard, T. (1983) *Biochim. Biophys. Acta 743*, 23−30.
3. Ronnberg, M., and Ellfolk, N. (1979) *Biochim. Biophys. Acta 581*, 325−333.
4. Gilmour, R., Goodhew, C. F., Pettigrew, G. W., Prazeres, S., Moura, I., and Moura, J. J. (1993) *Biochem. J. 294*, 745−752.
5. Hu, W., De Smet, L., Van Driessche, G., Bartsch, R. G., Meyer, T. E., Cusanovich, M. A., and Van Beeumen, J. (1998) *Eur. J. Biochem. 258*, 29−36.

6. Arciero, D. M., and Hooper, A. B. (1994) *J. Biol. Chem. 269*, 11878−11886.
7. Fulop, V., Ridout, C., Greenwood, C., and Hajdu, J. (1995) *Structure 3*, 1225−1233.
8. Sivaraja, M., Goodin, D. B., Smith, M., and Hoffman, B. M. (1989) *Science 245*, 738−740.
9. Dolphin, D., Forman, A., Borg, D. C., Fajer, J., and Felton, R. H. (1971) *Proc. Natl. Acad. Sci. U.S.A. 68*, 614−618.
10. Foote, N., Turner, R., Brittain, T., and Greenwood, C. (1992) *Biochem. J. 283*, 839−843.
11. Greenwood, C., Foote, N., Gadsby, M. A., and Thomson, A. J. (1988) *Chem. Scr. 28A*, 79−84.
12. Pappa, H., Li, H., Sundaramoorthy, M., Arciero, D., Hooper, A., and Poulos, T. L. (1996) *J. Struct. Biol. 116*, 429−431.
13. Navanza, J., and Saludjian, P. (1997) *Methods Enzymol. 276*, 581−594.
14. de La Fortelle, E., and Bricogne, G. (1996) *Methods Enzymol. 276*, 472−494.
15. Schuller, D. J. (1996) *Acta Crystallogr., Sect. D D52*, 425−434.
16. Bailey, S. (1994) *Acta Crystallogr., Sect. D D50*, 760−763.
17. Brunger, A. T., Adams, P. D., Clore, G. M., DeLano, W. L., Gros, P., Grosse-Kunstleve, R. W., Jiang, J. S., Kuszewski, J., Nilges, M., Pannu, N. S., Read, R. J., Rice, L. M., Simonson, T., and Warren, G. L. (1998) *Acta Crystallogr., Sect. D D54*, 905−921.
18. Jones, T. A. (1985) *Methods Enzymol.*, 157−171.
19. Sundaramoorthy, M., Terner, J., and Poulos, T. L. (1995) *Structure 3*, 1367−1377.
20. Sundaramoorthy, M., Terner, J., and Poulos, T. L. (1998) *Chem. Biol. 5*, 461−473.
21. Wagenknecht, H. A., and Woggon, W. D. (1997) *Chem. Biol. 4*, 367−372.
22. Williams, P. A., Fulop, V., Garman, E. F., Saunders, N. F., Ferguson, S. J., and Hajdu, J. (1997) *Nature*, 406−412.
23. Kraulis, P. J. (1991) *J. Appl. Crystallogr*, *24*, 946−950.
24. Esnouf, R. M. (1999) *Acta Crystallogr*., *Sect. D D55*, 938−940.
25. Merritt, E. A., and Bacon, D. J. (1997) *Methods Enzymol. 277*, 505−524.

BI011481H